Nikolaienko and Kryachko *Nanoscale Research Letters* (2015) 10:185
DOI 10.1186/s11671-015-0871-x

Nanoscale Research Letters
a SpringerOpen Journal

NANO REVIEW Open Access

Formation of dimers of light noble atoms under encapsulation within fullerene's voids

Tymofii Yu Nikolaienko[1] and Eugene S Kryachko[2*]

Abstract

Van der Waals (vdW) He_2 diatomic trapped inside buckminsterfullerene's void and preserving its diatomic bonding is itself a controversial phenomenon due to the smallness of the void diameter comparing to the He-He equilibrium distance. We propound a computational approach, including smaller fullerenes, C_{20} and C_{28}, to demonstrate that encapsulation of He_2 inside the studied fullerenes exhibits an interesting quantum behavior resulting in a binding at shorter, non-vdW internuclear distances, and we develop a computational model to interpret these He-He bonding patterns in terms of Bader's atom-in-molecule theory. We also conjecture a computational existence of $He_2@C_{60}$ on a solid basis of its theoretical UV absorption spectrum and a comparison with that of C_{60}.

Keywords: Fullerene confinement; Noble atoms dimers; Bonding patterns; QTAIM

Review

Background introduction

At the recent lecture of Prof. Ihor R. Yukhnovskii 'Phase Transition of the First Order Below the Liquid-Gas Critical Point', partly published elsewhere [1], one of the authors of the titled work, E.S.K., has been actually impressed by a great vitality of the ingenious idea that lay behind a very simple equation of state, which Johannes Diderik van der Waals derived in his PhD thesis in 1837 and which won him the 1910 Nobel Prize in Physics [2], and that spread over centuries, the idea of the attractive dispersion force referred, after him, to as the van der Waals force. This force is responsible for the correction to the pressure in this equation of state and governs myriads of interactions appearing between atoms and molecules in a variety of chemical and biochemical processes [3-7]. Nevertheless, this vitality of van der Waals (vdW) interactions lies actually in that they continue - even after 177 years - to wonder: three recent events will serve as good examples.

The spectroscopic detection of the weakly bound van der Waals diatomic LiHe has been reported [8] in 2013. Actually, this system was predicted 14 years earlier, as existing with a single bound rovibrational state in the $X^2\Sigma$ ground electronic state characterized by the average bond length of approximately 28 Å and the binding energy of 0.0039 cm^{-1} (approximately 0.56 mK) [9]. Another surprise came in 2000 when the diffraction experiments [10] of molecular beam consisting of small clusters of He finally resolved the longstanding paradox with the van der Waals $^4He_2$ dimer. The paradox - not yet then thought as that - started in 1931 when Slater and Krkwood performed the first calculation of the He-He potential [11], later corrected by Hirschfelder, Curtiss, and Bird in their famous book [12], and thoroughly reviewed by Margenau and Kestner [13], Hobza and Zahradnik [5], Kaplan [3], and Barash [14] (and the references therein, on the works of L. D. Landau school in particular). The importance of this interaction is hardly to overestimate since helium is the second most abundant element after hydrogen and the second simplest atom in the universe (see, e.g., [15]). The interaction between two helium atoms arises electrostatically, when an electric multipole on one atom creates a surrounding electric field that induces an electric mutipole moment on the other. In contrast to other molecular interactions, the van der Waals one is not related to a charge transfer - according to the Mulliken rule, the charge transfer is completely absent in the He-He interaction (see e.g., [16], p. 877) due to the enormous ionization potential of He equal to 24.5 eV, its small (in fact, negative) electron affinity, and very small polarizability $\alpha = 0.21$ $Å^3$. The latter make the He-He interaction extremely weak: the mean

* Correspondence: eugene.kryachko@ulg.ac.be
[2]Bogolyubov Institute for Theoretical Physics, 14-b, Metrolohichna str., Kyiv 03680, Ukraine
Full list of author information is available at the end of the article

He-He internuclear distance (the bond length, in a sense) reaches 52 ± 4 Å and its binding energy 1.1 mK [10] (≈0.0022 kcal/mol, compared to quantum chemical accuracy of approximately 1 kcal/mol [17]), thus providing, first, an unusual inertness of He: Toennies [15] mentioned that only 'a few compounds containing helium have been predicted [1], but none have been found,' and, second, the breakdown of the Born-Oppenheimer approximation. In this lies the idea of the aforementioned paradox.

Another surprise came out from an unexpected side, from fullerenes [18]: in 2009, Peng and Wang et al. [19] developed the explosion-based method and prepared the endohedral fullerene $He_2@C_{60}$, which existence was confirmed in their mass spectrum experiments. It is not, however, absolutely clear how C_{60} enables to accommodate He_2 dimer since its void diameter 0.7 nm = 7 Å is smaller than the aforementioned mean He-He internuclear distance, and thus, rules out that He_2 dimer is still bonded therein. These authors claimed that the He-He bonding in $He_2@C_{60}$ arises due to the following mechanism: the repulsive interaction between two helium atoms keeps them away from the center, thus approaching each to C_{60} surface and establishing a charge transfer between He and C_{60}. Altogether, this slightly distorts the C_{60} architecture that was detected in the peak recycling high performance liquid chromatography (HPLC) retention time. Only fewer computational works that have been done in parallel to this experiment mostly fell to agree with the latter and to explain it.

Our aim is to recover the agreement between experiment and theory by conducting a series of computations which include van der Waals effects and to offer the computational model behind the mechanism of bonding in $He_2@C_{60}$. The layout of the present work is the following. The 'Methodological strategy' section opens the methodological content of this work. The next section 'Results and discussion' focuses on discussing theoretical He-He and Ne-Ne bonding patterns and offers, and in the 'Notes: computational experiment' section, we give a definite computational evidence for the very existence of $He_2@C_{60}$ in terms of its theoretical UV absorption spectrum which is experimentally measurable. The work completes with thorough discussions and future perspectives.

Methodological strategy

All systems studied in the present work are divided into three categories: fullerenes, He- and Ne@fullerenes, and He_2- and Ne_2@fullerenes where the intermediate one is chosen as the reference origin to examine the He-He and Ne-Ne bondings in the last category.

Fullerenes

Fullerenes belong to the class of materials with a high ratio of surface to volume. According to the mathematical definition [20], *a fullerene is the surface of a simple closed convex 3D-polyhedron with only 5- and 6-gonal faces* (*pentagons and hexagons*). We assert that this surface/volume high ratio definitely predetermines a hollow cage architecture or void within a fullerene whose propensity is to accommodate (incapsulation or embedding) therein guest atom(s) or molecule(s) [21]. The latter system with the fullerene doped by atom is nowadays dubbed, after Cioslowski [22] and Schwarz and Krätschmer [23], as an 'endohedral fullerene' that originates from Greek words *ενδον* ('endon' - within) and *εδρα* ('hedra' - face of geometrical figure) [21].

The present work extends a class of He_2@fullerenes to a variety of fullerenes that begins from the smallest C_{20} [24], intermediate C_{28} [25-27], and ends at the famous buckminsterfullerene C_{60} [18]. All of them are displayed in Figure 1 together with the invoked computational levels. The latter consist of two approaches based on the density functional (see e.g., [28] and references therein) and wave function (*ab initio*) theories. Notice that, according to [29], the MP2 and B3LYP predictions are very similar.

He@fullerenes and He_2@fullerenes Endofullerenes with encapsulated noble gas (Ng) atoms have been scarcely studied in the past, both experimentally and theoretically, compared to the first endohedral metallofullerene (EMF) $La@C_{82}$, isolated in 1991 [30]. The reason is in that the Ng-encapsulation has very low yields and features a rather tedious separation from the host fullerene [21]. Though, the experiments on high-temperature decomposition of $Ng@C_{60} \Rightarrow Ng + C_{60}$ have revealed the activation barrier of ca. 90 kcal·mol^{-1} high [31,32] (see also [33]). On the theoretical side, it is worth mentioning the second-order Møller-Plesset perturbation and density functional computational approaches [29,33,34] to study Ng-endohedral complexes with C_{60}-buckminsterfullerene [29,33,34] (see [21,35] for current reviews and references therein).

In the present work, Ng@fullerenes (Ng = He, Ne) and Ng_2@fullerenes were studied at the same computational level as their cage fullerenes (see Figure 1). To reveal the bonding patterns in the He_2@fullerenes, Bader's 'atoms-in-molecules' (AIM) theory [36-38] was invoked since it provides a mathematically elegant approach [37] to describe a bonding. It should be noted beforehand that the theme on a chemical bond is rather fragile and subtle (see, e.g., Introduction in [39] and references therein). Once Bader [36] conjectured that one-electron density $\rho(\mathbf{r})$, $\mathbf{r} \in \mathbb{R}^3$ of a given molecule should contain the essence of this molecule's structure. Precisely, the topology of density is characterized by introducing the corresponding gradient vector field $\nabla_{\mathbf{r}}\rho(\mathbf{r})$ given by a bundle of trajectories as curves $\mathbf{r} = \mathbf{r}(s)$ parametrized by some

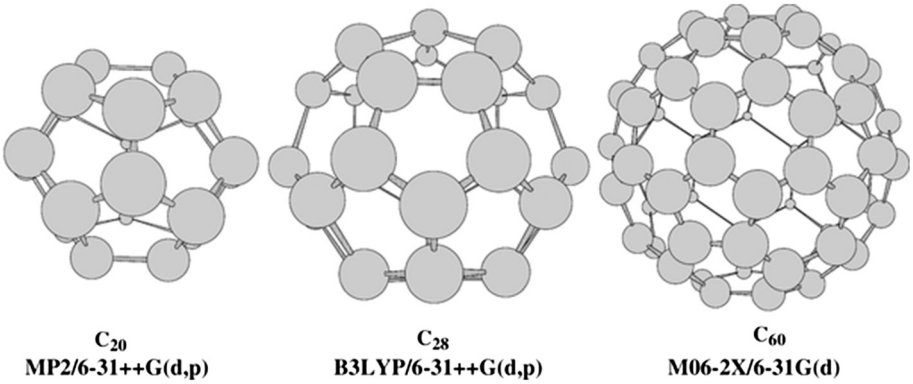

Figure 1 Studied fullerenes. Below their structures are indicated the corresponding computational levels invoked in the present work using Gaussian-09 package of programs [64] (keyword Int = UltraFine was invoked). C_{20} is the smallest fullerene consisting of 12 pentagons. Its HOMO-LUMO gap amounts to 0.96 eV [24]. C_{28} has a *Td* symmetry [25,26] and generates actually the smallest endohedral fullerenes M@C_{28} with M = Ti, Zr, and U [26,27]. For C_{60}, we employ the M06-2X meta exchange-correlation density functional which takes into account a vdW-correction [65,66] and which was recently used in [67] for analogous tasks. As known, C_{60} consists of 12 pentagons and 20 hexagons. Each carbon forms a single double bond with the C-C bond length of 1.404 Å and two single bonds of 1.448 Å (note: MP2 ones are equal to 1.406 and 1.446 Å, respectively [68]).

parameter s and satisfying the equation $d\mathbf{r}(s)/ds = \nabla_{\mathbf{r}}\,\rho(\mathbf{r}(s))$. The trajectories with zero gradient defines the zero-flux surface $\partial\Omega$: = $\{\mathbf{r} \in \mathbb{R}^3 |\ \mathbf{n}(\mathbf{r}) \cdot \nabla_{\mathbf{r}}\,\rho(\mathbf{r}) = 0$, where $\mathbf{n} = \mathbf{r}/|\mathbf{r}|\}$. This surface bounds a region in $\mathbb{R}^3$ that defines a (topological) 'atom', or atomic basin. Two atoms are defined as *bonded* if they share a common interatomic surface. If follows from topology that each zero-flux surface contains a (3,−1)-type critical point $\mathbf{r}_c \in \mathbb{R}^3$ (CP) where $\nabla_{\mathbf{r}}\rho(\mathbf{r}_c) = 0$ and where the Hessian matrix of ρ has two negative and one positive eigenvalues. The eigenvector of this Hessian matrix corresponding to its positive eigenvalue define two directions in which two trajectories of the $\nabla_{\mathbf{r}}\rho$-field originate from the critical point forming a so-called 'bond path' connecting two attractors (which typically are atomic nuclei).

It is worth noticing that although AIM itself provides only a *definition* of a topological atom and does not provide a formal proof for its relevance to 'chemical' atoms, numerous examples demonstrate the fruitfulness of equating these concepts. In particular, bond paths have been shown to be a universal indicator of bonded interactions [40,41]. In the latter context, AIM is used in this work. Using Gaussian package, we obtained the electron density distributions at the corresponding computational level using the keyword 'output = wfn' and analyzed it with AIMAll package [42] to reveal all (3,−1)-type critical points and bond paths of the electron charge density distribution. A bond ellipticity that defines a measure of the extent to which a charge is preferentially accumulated in a given plane [30] was calculated as $\varepsilon = \lambda_1/\lambda_2 - 1$, where λ_1 and λ_2 are negative eigenvalues ($|\lambda_1| \geq |\lambda_2|$) of the Hessian matrix $H_{ij} = \frac{\partial^2 \rho}{\partial x_i \partial x_j}$ $(i,j = 1,2,3)$ evaluated at the bond critical point. When possible transformations of a given molecular graph represented by a set of molecular bond paths are considered, it can be shown that 'the ellipticity of the bond which is to be broken increases dramatically and becomes infinite at the geometry of the bifurcation point' so that 'a structure possessing a bond with an unusually large ellipticity is potentially unstable' [37]. Therefore, the value of bond ellipticity can be considered as the measure of bond stability.

In conclusion, naturally anticipating the contribution of a vdW force into the bonding of the titled endofullerenes (see e.g., [43]), we also employed the ORCA package [44,45] using the density-dependent, non-local dispersion functional of Vydrov and Van Voorhis [46] in conjunction with the Ahlrichs' TZV(2d,2p) polarization functions. Time-dependent DFT [47] was invoked within this package to calculate UV absorption spectra of C_{60} and $He_2@C_{60}$.

Results and discussions

The resulted structures of the studied He_2@fullerenes together with some geometrical details are presented in Figure 2. We therefore envisage the following physics behind embeddings of the He_2 diatomic into the voids of C_{20}, C_{28}, and C_{60} fullerenes. Let, for clarity and simplicity, limit ourselves by C_{60} and a single He atom.

Solid lines depict covalent bonds, whereas the dashed ones connect the atoms linked by a bond path according to the AIM analysis of the electron density distributions. q_{Ng} designates the Mulliken atomic charge of the Ng atom. The asterisk indicates the ORCA's Mulliken gross atomic charge. Representative bond distances of the considered systems are presented in Table 1. $\bar{R}$ (in Å) is the

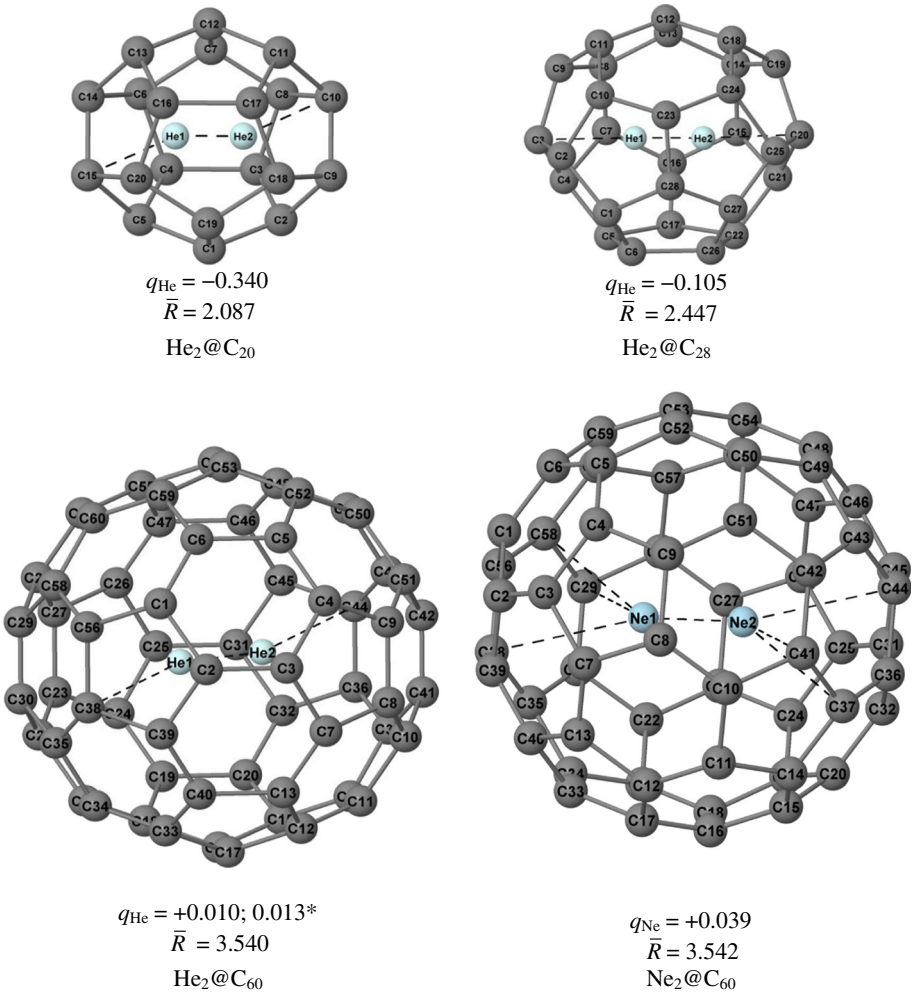

Figure 2 The calculated structure of endohedral fullerene $Ng_2@C_{20},C_{28},C_{60}$ (Ng = He, Ne), together with its atomic numbering.

root-mean-square radii, $\bar{R} = \sqrt{\frac{1}{N}\sum_{i=1}^{N} R_i^2}$ (where R_i is the distance from the geometrical center to the *i*th carbon atom), of a given endofullerene with N carbon atoms: $\bar{R}$ (C_{20}) = 2.036 Å, $\bar{R}$ (C_{28}) = 2.427 Å, and $\bar{R}$ (C_{60}) = 2.540 Å.

The thought scenario of embedding of He into the C_{60} void from outside (a so-called exo-fullerene HeC_{60}) includes a passage of He through a rather high barrier which profile is shown in Figure 3. This barrier of approximately 300 kcal/mol is rather high and ensures, on the one hand, a very large lifetime of $He@C_{60}$. On the other hand, generalizing this barrier over the total fullerene surface, it obviously results in a confining void or confinement characterized by a high potential wall that ultimately results in a kinetic stability of $He@C_{60}$ and its very large (practically infinite) lifetime, according to the transition-state theory (see e.g., [48] and references therein), though the recent calculations invoking PBE density functional with inclusion of the D3-type dispersion corrections [49] demonstrate a relatively weak binding of –2.434 kcal/mol.

Lets imagine that at the next stage, the second He atom is added to the endohedral fullerene He@C60 with a single encapsulated atom of He. From Figure 2, it follows that the embedding of Ng_2 (Ng = He, Ne) into buckminsterfullerene causes its slight swelling, indicated by $\bar{R}$, and a charge transfer from Ng_2 to C_{60}; however, the Mulliken charge q_{Ng}, which measures this charge transfer, varies in fractions rather than in integers - note that variations of similar magnitude were observed in the work [50]. We suggest that a so-called ionic conjecture or the ionic model [21,35,51,52] is capable to explain this charge transfer by analogy with that taking place in EMF. In both cases, the host fullerene plays a role of an electron buffer [53]. Physics behind the charge transfer in $He_2@C_{60}$ is the following: approaching two ground-state atoms, say A and B, of He, whose two

Table 1 Data of the AIM analysis of the electron density distribution in $Ng_2@C_{60}$ (Ng = He, Ne)

Bond (A ⋯ B)	R_{AB}, Å	$\rho^{cp} \cdot 10^2$, e/a_B^3	Bond ellipticity
$He_2@C_{60}$			
$He_1 \cdots He_2$	1.979[a,b]	1.26	$3 \cdot 10^{-6}$
$C_{38} \cdots He_1$	2.588	1.07	1.21
$C_{44} \cdots He_2$	2.588	1.07	1.21
$He_2^+(^2\Sigma_u^+)$:			
Present work	1.1881[c]		
MR-CI [69]	1.0816		
B3LYP [56]	1.1454[d,e]		
Expt. [57-59]	1.0806[f]		
$Ne_2@C_{60}$			
C38 ⋯ Ne1	2.649	1.57	8.31
C58 ⋯ Ne1	2.631	1.63	10.46
C29 ⋯ Ne1	2.638	1.60	5.53
C41 ⋯ Ne2	2.638	1.60	5.53
C37 ⋯ Ne2	2.631	1.63	10.46
Ne1 ⋯ Ne2	2.096	3.40	$6 \cdot 10^{-5}$
C44 ⋯ Ne2	2.649	1.57	8.31
C38 ⋯ Ne1	2.649	1.57	8.31

R_{AB} is the A ⋯ B-internuclear distance, $\rho^{cp} \equiv \rho(r_{CP})$, the charge density at the (3, −1) bond critical point (CP), and a_B is the Bohr radius. ρ^{cp} qualitatively measures a strength of a non-covalent interaction. [a]Other computational levels: BP86/TZVPP: 1.948 [39]; M05-2X/6-311G(d): 2.035 [70]. [b]ν(He-He) stretch in $He_2@C_{60}$ is centered at 531.0 cm^{-1}. [c]The calculated frequency in He_2^+ is equal to 1293 cm^{-1}. [d] ν(He-He) stretch = 1359.9 cm^{-1}. [e] ν(He-He) stretch = 1192.8 cm^{-1}. [f] ν_{expt}(He-He) stretch = 1698.5 cm^{-1} [57-59].

electrons occupy $1s_{He}$ atomic orbital, to each other results in formation of the bonding molecular orbital (MO) $1s\sigma_g$ and the antibonding MO $1s\sigma_u^*$ (see Figure 4 and also [54]). The latter that is stronger, MO$1s\sigma_g$, overlaps the LUMO (hole) of C_{60} that promotes a charge transfer $He1s\sigma_u^* \Rightarrow C_{60}$ –hole - the corresponding internuclear distances of 1.68 Å (Table 1) are smaller, a sum of the vdW radii which are equal to 1.4 Å for He and 1.7 Å for carbon, respectively [55]. This weakens the MO $1s\sigma_u$ and, in turn, strengthens the bonding interaction MO $1s\sigma_g$, converting He_2 into fractionally ionized $[He\text{-}He]^{+0.02}$ moiety. AIM properties of the latter subsystem are summarized in Table 1.

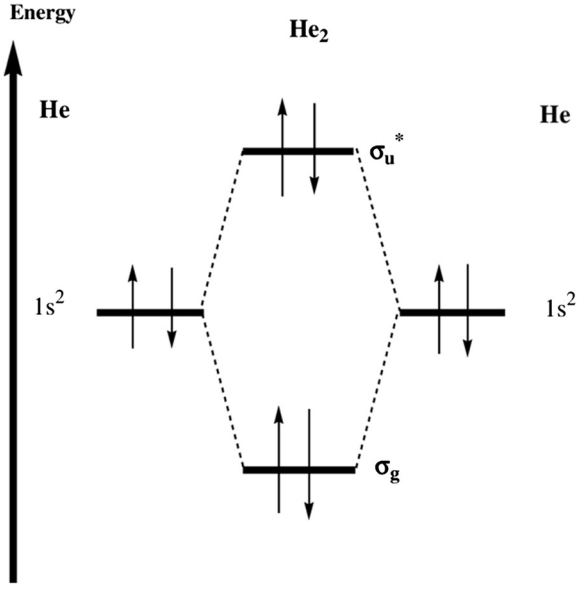

Figure 4 Formation of the bonding molecular orbital (MO) $1s\sigma_g$ and the antibonding MO $1s\sigma_u^*$.

Interestingly, the He-He bond length in $[He\text{-}He]^{+0.02}@C_{60}^{-0.02}$ contracts to 1.175 Å that is considerably smaller than the vdW-bond length in the He_2 dimer. On the other hand, it rather well correlates with the equilibrium distance of the ground-state dihelium cation He_2^{+1} equal to

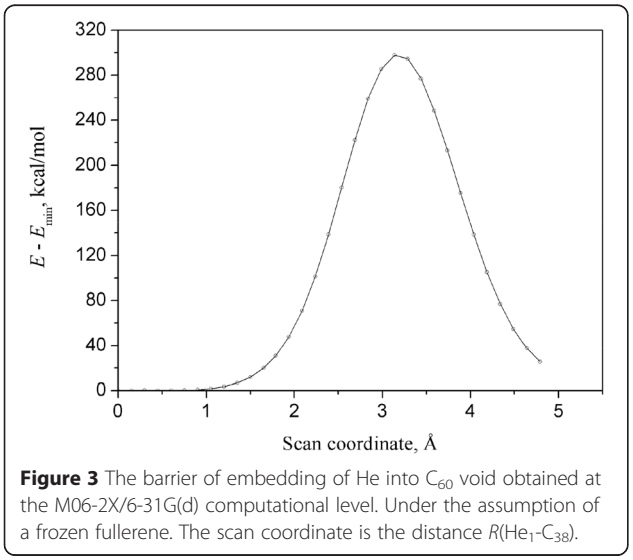

Figure 3 The barrier of embedding of He into C_{60} void obtained at the M06-2X/6-31G(d) computational level. Under the assumption of a frozen fullerene. The scan coordinate is the distance $R(He_1\text{-}C_{38})$.

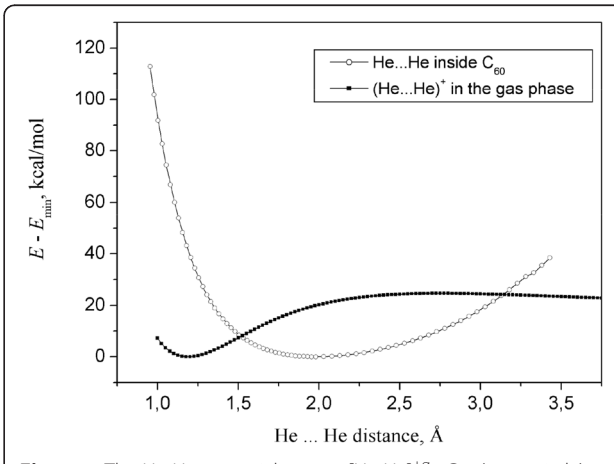

Figure 5 The He-He potential curves: $[He\text{-}He]^{+q}@C_{60}$ (open circle); the ground-state dihelium cation He_2^+ (filled circle; insert).

1.2206 Å (cf. with the experimental value of 1.0806 Å [56-59]) obtained at the B3LYP/6-31G(d) computational level in the present work. We anticipate such behavior: the larger electron charge q $(0 \le q \le 1)$ is removed from MO $1s\sigma_u^*$, the stronger is bonding in $[He\text{-}He]^{+q}@C_{60}^{-q}$. We continue this comparison of $[He\text{-}He]^{+q}$ moiety embedded into C_{60} with the dihelium cation He_2^{+1} in Figure 5 by comparing their He-He potential curves.

Finally, one can conclude from Table 1 and Figure 5 that in all studied complexes the He ⋯ He bond is much stronger than that between He and carbon atoms of the fullerene. In this regard, let us compare the He-He

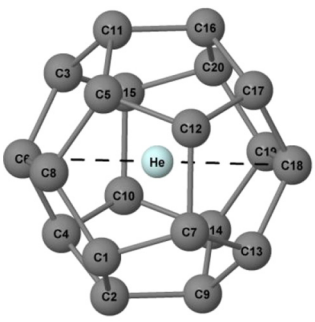

q_{He} = -0.240
$\overline{R}$ = 2.051 vs. 2.036 Å
He@C_{20}

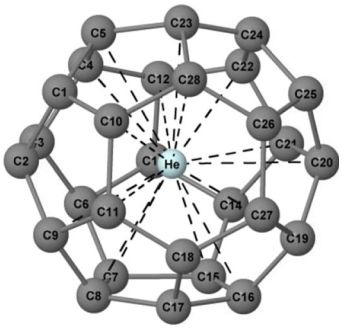

q_{He} = -0.160
$\overline{R}$ = 2.431 vs.2.427 Å
He@C_{28}

Bond (A⋯B)	R_{AB}, Å	$\rho^{cp} \cdot 10^2$, e/a_B^3	Bond ellipticity
He@C_{20}			
C6⋯He	1.984	3.94	$2 \cdot 10^{-3}$
C18⋯He	1.984	3.94	$2 \cdot 10^{-3}$
He_2@C_{20}			
He1⋯He2	1.175	13.69	$4 \cdot 10^{-3}$
C15⋯He1	1.681	8.23	11.6
C10⋯He2	1.681	8.23	11.6
He@C_{28}			
C5⋯He	2.413	1.62	0.85
C4⋯He	2.401	1.58	1.48
C7⋯He	2.420	1.52	0.71
C9⋯He	2.428	1.52	1.77
C8⋯He	2.448	1.52	4.09
C11⋯He	2.428	1.52	1.79
C12⋯He	2.425	1.52	4.02
C15⋯He	2.371	1.64	1.82
C16⋯He	2.413	1.62	0.83
C10⋯He	2.448	1.52	3.58
C21⋯He	2.408	1.58	2.63
C19⋯He	2.400	1.58	1.44
C23⋯He	2.371	1.64	1.81
C28⋯He	2.419	1.52	0.71
C22⋯He	2.408	1.58	2.64
C20⋯He	2.424	1.52	4.01
He_2@C_{28}			
He1⋯He2	1.359	7.47	0.99
C3⋯He1	1.897	4.63	$9 \cdot 10^{-5}$
C20⋯He2	1.897	4.63	0.99

Figure 6 Characteristics of non-covalent interactions in Ng@C_{20} and Ng@C_{28} (Ng = He, He_2) endofullerene complexes (for notations, see Figure 2 and Table 1).

stretching mode $\nu_{\text{He-He}}$ in the studied endofullerene with $\nu^{\text{expt}}_{\text{He-He}} = 1{,}698.5\ \text{cm}^{-1}$ of the dihelium cation [57-59]: (a) in $[\text{He-He}]^{+0.02}@C_{60}^{-0.02}$ $\nu_{\text{He-He}}$ contributes to the collective modes centered at 495.7, 504.8, and 531 cm^{-1}. Note, for a purpose of comparison, that (b) in $He_2@C_{20}$ $\nu_{\text{He-He}}$ peaks at 2,380.6 cm^{-1}, whereas in $He_2@C_{28}$ $\nu_{\text{He-He}}$ peaks at 1,682.1 cm^{-1}; and (c) in $[\text{Ne-Ne}]^{+0.08}@C_{60}^{-0.08}$ contributes to the collective modes centered at 440.6, 458.2, and 519.4 cm^{-1}. A peculiar feature of $\text{He}\cdots\text{C}$ bond, especially in $He_2@C_{20}$ complex, is a rather large magnitude of ellipticity which, along with symmetry considerations, probably indicates that $\text{He}_1\cdots\text{C}_{14}$ and $\text{He}_2\cdots\text{C}_9$ bonds could also exist in $He_2@C_{20}$ complex (see Figure 2).

Some representative properties of $Ng_2@C_{20}$ and $Ng_2@C_{28}$ are collected in Figure 6 where we add those for trapping a single noble-gas atom. Clearly, compared to $Ng_2@C_{60}$, the encapsulation of Ng_2 into smaller C_{20} and C_{28} is governed by many other effects among which are worth noticing the steric effect and the following one:

- Overlap of the asymptotic tails of the electron densities of carbon atoms with that of He that may lead to negative Mulliken charges q_{He} since the corresponding internuclear distances of 1.98 and 2.37 Å are smaller than the sum of the vdW radii which are correspondingly equal to 1.4 for He and 1.7 Å for carbon [52]. To shed a light on this mechanism, we performed some additional calculations for the same complex geometries with the He atom replaced by the 'ghost' (defined as the 'atom' with the same set of basic functions and the zero nuclear charge). They show that (i) in $He@C_{20}$, the 'ghost' He charge is −0.358 (vs. −0.240 for real atom) so that insertion of a single He into a void of C_{20} results in overlapping of electronic clouds and thus to negative Mulliken charge on helium; (ii) in $He_2@C_{20}$, the 'ghost' He atom acquires a Mulliken charge of −0.101 (cf. −0.340 for real atoms). It should be noted however that each of He_2 atoms lies apart further from the center of C_{20} void as compared to the situation with the single He atom [28], so that the charge repelled by He_1 can, in principle, induce an increase of population on He_2 and vice versa.

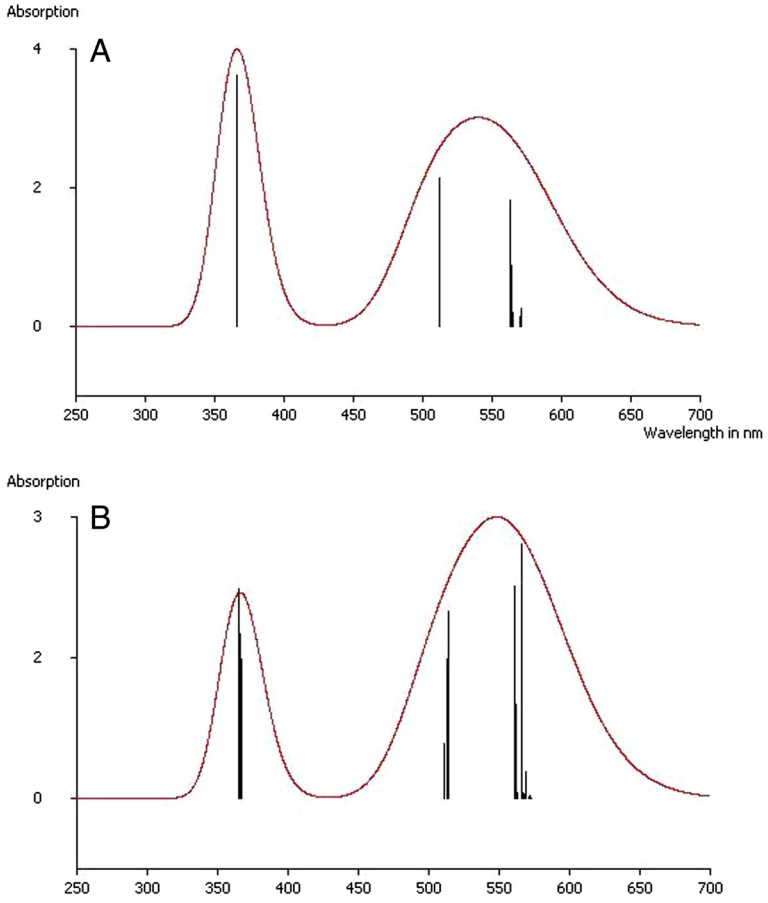

Figure 7 The UV absorption spectra: $He_2@C_{60}$ (top) and C_{60} (bottom) calculated within the TD DFT (width σ = 0.2 eV).

Notes: computational experiment

It is natural to view any computational model as a kind of experimental one, and hence, to extend all requirements, we usually impose on an experiment, on in its 'computational' cousin. Among them, one is reproducibility, the other is that an experiment should be treated as a test of a model or theory, and the third is the experiment's capability to produce new data serving to test a given theoretical model. In the present work, the latter was chosen in the spectroscopic field: it is the UV absorption spectrum of $He_2@C_{60}$ system obtained in the present work using the TD DFT implemented in ORCA and presented in Figure 7 for its comparison with that of C_{60} by a straightforward analogy with the corresponding experimental spectrum, there are a strong peak around 300 nm and a very broad absorption between 450 and 600 nm [60]. Therefore, we may definitely conclude that if such the difference in the spectra of $He_2@C_{60}$ system and of C_{60} is experimentally observed, it is a solid argument in favor of the ionic mechanism of He_2 bonding inside C_{60}.

Glancing over Figure 7, our first impression is that the UV absorption spectra of $He_2@C_{60}$ system and of C_{60} are quite similar: two peaks, one is narrow, the other is quite broad - and such similarity we have already observed in the UV spectra of $Kr@C_{60}$, also isolated by HPLC, and C_{60} [21,61]. On the other hand, this similarity emphasizes a distinguished difference of the studied UV spectra and therefore, the way to experimentally discriminate between the corresponding systems, $He_2@C_{60}$ and C_{60}.

Conclusions

After 30 years since the serendipitous discovery of fullerenes by Sir Kroto and co-workers [62], let us recall the statement by Ashcroft [63] that 'The issue for C60 seems to go deeper.' This is precisely what has been done in the present work which provides a solid computational basis for the existence of the buckminsterfullerene with the van-der-Waals-bonded He dimer which has been recently isolated in the HPLC experiments. A variety of its computational properties, from spectroscopic to the bonding ones, calculated by invoking Bader's 'atoms-in-molecules' quantum theory, have been discussed and presented to identify its experimental 'fingerprints' and to reveal the mechanism of its bonding after trapping of He_2 inside C_{60}.

Competing interests

The authors declare that they have no competing interests.

Authors' contributions

TN carried out the AIM analysis and characterization of the calculated structures of fullerenes and endofullerenes and built the tables. ESK participated in the computational works, analyzed the results, and completed the first draft of the manuscript. ESK supervised the research. Both authors read and approved the final manuscript.

Acknowledgements

We thank the GRID computational facilities of the Bogolyubov Institute for Theoretical Physics for the excellent computational service. One of the authors, ESK, would like to acknowledge stimulating discussions with Sigrid Peyerimhoff and Stefan Grimme. This work was supported by the Research Grant of the Alexander von Humboldt Foundation and conducted within the Programme 'Microscopic and Phenomenological Models of Fundamental Physical Processes in Micro- and Macro-Worlds' of the Division of Physics and Astronomy (PR No. 0112U000056), Natl. Acad. Sci. Ukraine.
Note: After submission of this work, one of the present authors, ESK, received a copy of the 2015th paper [54] which systematically studied the encapsulation of rare-gas atoms into a series of fullerenes, from C_{20} to C_{60}, using the dispersion-corrected DFT.

Author details

[1]Faculty of Physics, Taras Shevchenko National University of Kyiv, 64/13, Volodymyrska Street, Kyiv 01601, Ukraine. [2]Bogolyubov Institute for Theoretical Physics, 14-b, Metrolohichna str., Kyiv 03680, Ukraine.

Received: 20 October 2014 Accepted: 20 March 2015
Published online: 17 April 2015

References

1. Yukhnovskii IR, Kolomiets VO, Idzyk IM. Liquid-gas phase transition at and below the critical point. Condens Matter Phys. 2013;16:1–6.
2. van der Waals JD, The Nobel Prize in Physics 1910. Nobelprize.org. Nobel Media AB. http://www.nobelprize.org/nobel_prizes/physics/laureates/1910/. Accessed 12 April 2015
3. Kaplan IG. Introduction to theory of intermolecular interactions. Nauka, Moscow: John Wiley & Sons; 1982. p. 20. in Russian.
4. Kaplan IG. Intermolecular interactions: physical picture, computational methods and model potentials. Chichester: Wiley; 2006.
5. Hobza P, Zahradnik R. Intermolecular complexes. Prague: Academia; 1988.
6. Israelachvili JN. Intermolecular and surface forces. London: Academic; 1985. Section 2.4.
7. Kipnis AY, Yavelov BE, Rowlinson JS. van der Waals and molecular sciences. New York: Oxford; 1996.
8. Tariq N, Taisan NA, Singh V. Weinstein J D. Phys Rev Lett. 2013;110:153201.
9. Kleinekathöfer U, Lewerenz M, Mladenović M. Phys Rev Lett. 1999;83:4717.
10. Grisenti RE, Schöllkopf W, Toennies JP, Hegerfeldt GC, Köhler T, Stoll M. Determination of the bond length and binding energy of the helium dimer by diffraction from a transmission grating. Phys Rev Lett. 2000;85:2284–7.
11. Slater JC, Kirkwood JG. The van der Waals forces in gases. Phys Rev. 1931;37:682–97.
12. Hirschfelder JE, Curtiss CF, Bird RB. Molecular theory of gases and liquids. N. Y: Wiley; 1954.
13. Margenau H, Kestner NR. Theory of intermolecular forces. N. Y.: Pergamon; 1971.
14. Barash Yu S, van der Waals Forces (in Russian), Nauka, Moscow, 1988.
15. Toennies JP. Helium clusters and droplets: microscopic superfluidity and other quantum effects. Mol Phys. 2013;111:1879.
16. Collins JR, Gallup GA. Contributions to interatomic and intermolecular forces. II. Interaction energy of two He atoms. Mol Phys. 1983;49:871–9.
17. Morokuma K. New challenges in quantum chemistry - quests for accurate calculations for large molecular systems. Phil Trans Roy Soc Lond A. 2002;360:1149–64.
18. Kroto HW, Heath JR, O'Brien SC, Curl RF, Smalley RE. C_{60}: buckminsterfullerene. Nature. 1985;318:162-.
19. Peng R-F et al. Preparation of He@C60 and He2@C60 by an explosive method. J Mat Chem. 2009;19:3602–5.
20. Deza M, Sikiric MD, Shtogrin MI. Fullerenes and disk-fullerenes. Russian Math Surv. 2013;68:665–720.
21. Popov AA, Yang S, Dunsch L. Endohedral fullerenes. Chem Rev. 2013;113:5989–6113.
22. Cioslowski J, Fleischmann ED. Endohedral complexes: atoms and ions inside the C_{60} cage. J Chem Phys. 1991;94:3730–4.

23. Weiske T, Böhme DK, Hrusak J, Krätschmer W, Schwarz H, Angew. Endohedral cluster compounds: inclusion of helium within C_{60}^{+} and C_{70}^{+} through collision experiments. Chem Int Ed Engl. 1991;30:884–7.
24. Roland C, Larade B, Taylor J, Guo H. *Ab initio* I-V characteristics of short C20 chains. Phys Rev B. 2001;65:041401(R).
25. Fowler PW, Manolopoulos DE. An atlas of fullerenes. Oxford: Clarendon; 1995.
26. Makurin Yu N, Sofronov AA, Gusev AI, Ivanovsky AL. Electronic structure and chemical stabilization of C28 fullerence. Chem Phys. 2001;270:293–308.
27. Dunk PW, Kaiser NK, Mulet-Gas M, Rodriguez-Fortea A, Poblet JM, Shinohara H, et al. The smallest stable fullerene M@C28 (M = Ti, Zr, U). J Am Chem Soc. 2012;134:9380–9.
28. Kryachko ES, Ludeña EV. Density functional theory: foundations reviewed. Phys Rep. 2014;544(2):123–239.
29. Darzynkiewicz R, Scuseria GE. Noble gas endohedral complexes of C_{60} buckminsterfullerene. J Phys Chem A. 1997;101:7141–4.
30. Chai Y, Guo T, Jin CM, Haufler RE, Chibante LPF, et al. Fullerenes with metals inside. J Phys Chem. 1991;95:7564–8.
31. Shimshi R, Khong A, Jiménez-Vázquez HA, Cross RJ, Saunders M. Release of noble gases from inside fullerenes. Terahedron. 1996;52:5143.
32. Saunders M, Jiménez-Vázquez HA, Cross RJ, Poreda RJ. Stable compounds of helium and neon: He@C_{60} and Ne@C_{60}. Science. 1993;259:1428–30.
33. Ramachandran CN, Roy D, Sathyamurthy N. Host-guest interaction in endohedral fullerenes. Chem Phys Lett. 2008;461:87–92.
34. Patchkovskii S, Thiel W. Equilibrium yield for helium incorporation into buckminsterfullerene: quantum-chemical evaluation. J Chem Phys. 1997;106:1796–9.
35. Rodriguez-Fortea A, Irle S, Poblet JM. Fullerenes: formation, stability, and reactivity. WIREs Comput Mol Sci. 2011;1:350–66.
36. Bader RFW. Atoms in molecules: a quantum theory. Oxford: Oxford University Press; 1994.
37. Bader RF. A quantum theory of molecular structure and its applications. Chem Rev. 1991;1991(91):893–928.
38. Matta CF, Boyd RJ. Chapter 1. In: Matta CF, Boyd RJ, editors. The quantum theory of atoms in molecules. Weinheim: Wiley; 2007. p. 1–34.
39. Krapp A, Frenking G. Is this a chemical bond? A theoretical study of Ng2@C60 (Ng = He, Ne, Ar, Kr, Xe). Chem Eur J. 2007;13:8256–70.
40. Guo J, Ellis DE, Bader RFW, MacDougall PJ. Topological analysis of the charge density response of a Ni_4 cluster to a probe H_2 molecule. J Cluster Sci. 1990;1:201–21.
41. Bader RF. A bond path: a universal indicator of bonded interactions. J Phys Chem A. 1998;102:7314–23.
42. Keith T A, AIMAll (Version 14.04.17), TK Gristmill Software, Overland Park KS, USA. http://aim.tkgristmill.com. Accessed 12 April 2015
43. Pyykko P, Wang C, Straka M, Vaara J. A London-type formula for the dispersion interactions of endohedral A@B systems. Phys Chem Chem Phys. 2007;9:2954–8.
44. Neese, F, ORCA - an *ab initio*, DFT and semiemprical SCF-MO package (Version 2.9.1), University of Bonn, Bonn, Germany. https://orcaforum.cec.mpg.de/. Accessed 1 November 2012
45. Grimme S. Accurate description of van der Waals complexes by density functional theory including empirical corrections. J Comput Chem. 2004;25:1463–76.
46. Vydrov OA, Van Voorhis TJ. Nonlocal van der Waals density functional: the simpler the better. Chem Phys. 2010;133:244103 (originally termed VV10).
47. DeBeer-George S, Petrenko T, Neese F. Time-dependent density functional calculations of ligand K-edge X-ray absorption spectra. Inorg Chim Acta. 2008;361:965–72.
48. Deleuze MS, Francois J-P, Kryachko ES. The fate of dicationic states of molecular clusters of benzene and related compounds. J Am Chem Soc. 2005;127:16824–34.
49. Sure R, Tonner R, Schwerdtfeger P. A systematic study of rare gas atoms encapsulated in small fullerenes using dispersion corrected density functional theory. J Comput Chem. 2015;36:88–96.
50. Cheng C, Sheng L. Ab-initio study of helium-small carbon cage systems. Int J Quantum Chem. 2013;113:35–8.
51. Kobayashi K, Nagase S. Structures and electronic states of M@C_{82} (M = Sc, Y and La). Chem Phys Lett. 1998;282:325–9.
52. Popov AA, Dunsch L. Bonding in endohedral metallofullerenes as studied by quantum theory of atoms in molecules. Chem Eur J. 2009;15:9707–29.
53. Pavanello M, Jalbout AF, Trzaskowski B, Adamowicz L. Fullerene as an electron buffer: charge transfer in Li@C_{60}. Chem Phys Lett. 2007;442:339–43.
54. Bader RFW. An introduction to the electronic structure of atoms and molecules. Toronto: Clarke Irwin & Co Ltd; 1970. Ch. 6.
55. Pauling L. The nature of the chemical bond. 3rd ed. Ithaca, NY: Cornell University Press; 1960.
56. Bally T, Sastry GN. Incorrect dissociation behavior of radical ions in density functional calculations. J Phys Chem A. 1997;101:7923–5.
57. Huber KP, Herzberg G. Constants of diatomic molecules. N. Y: Van Nostrand Reinhold; 1979.
58. Frenking G, Cremer D. The chemistry of noble gas elements helium, neon, and argon - the experimental facts and theoretical predictions. Struct Bond. 1973;73:17–93.
59. Balanarayan P, Moiseyev N. Strong chemical bond of stable He_2 in strong linearly polarized laser fields. Phys Rev A. 2012;85:032516.
60. Lieber CM, Chen C-C. Preparation of fullerenes and fullerene-based materials. Solid State Physics. 1994;48:109–48.
61. Yamamoto K et al. Isolation and spectral properties of Kr@C60, a stable van der Waals molecule. J Am Chem Soc. 1999;121:1591–6.
62. Kroto HW, Heath JR, O'Brien SC, Curl RF, Smalley RE. C_{60}: buckminsterfullerene. Nature. 1985;318:162–3.
63. Ashcroft NW. Elusive diffusive liquids. Nature. 1993;365:387–8.
64. Frisch MJ, Trucks GW, Schlegel HB, Scuseria GE, Robb MA, et al. Gaussian 09, Revision A.02, Gaussian, Inc., Wallingford CT, 2009.
65. Zhao Y, Truhlar DG. The M06 suite of density functionals for main group thermochemistry, thermochemical kinetics, noncovalent interactions, excited states, and transition elements: Two new functionals and systematic testing og our M06-class functionals and 12 other functionals. Theor Chem Acc. 2008;120:215–41.
66. Zhao Y, Truhlar DG. Density functionals with broad applicability in chemistry. Acc Chem Res. 2008;41:157–67.
67. Tishchenko O, Truhlar DG. Atom-cage charge transfer in endohedral metallofullerenes: trapping atoms within a sphere-like ridge of avoided crossings. J Phys Chem Lett. 2013;4:422–5.
68. Häser M, Almlöf J, Scuseria GE. The equilibrium geometry of C_{60} as predicted by second-order (MP2) perturbation theory. Chem Phys Lett. 1991;181:497–500.
69. Cencek W, Rychlewski J. Many-electron explicitly correlated Gaussian functions. II. Ground state of the helium molecular ion He_2^+. J Chem Phys. 1995;102:2533–8.
70. Khatua M, Pan S, Chattaraj PK. Movement of Ng2 molecules confined in a C60 cage: an *ab initio* molecular dynamics study. Chem Phys Lett. 2014;610-611:351–6.